

An N^5 -scaling excited-state-specific perturbation theory

Rachel Clune,¹ Jacqueline A. R. Shea,¹ and Eric Neuscamman^{1, 2, a)}

¹⁾*Department of Chemistry, University of California, Berkeley, California 94720, USA*

²⁾*Chemical Sciences Division, Lawrence Berkeley National Laboratory, Berkeley, CA, 94720, USA*

(Dated: 14 January 2022)

We show that by working in a basis similar to that of the natural transition orbitals and using a modified zeroth order Hamiltonian, the cost of a recently-introduced perturbative correction to excited state mean field theory can be reduced from seventh to fifth order in the system size. The (occupied)²(virtual)³ asymptotic scaling matches that of ground state second order Møller-Plesset theory, but with a significantly higher prefactor because the bottleneck is iterative: it appears in the Krylov-subspace-based solution of the linear equation that yields the first order wave function. Here we discuss the details of the modified zeroth order Hamiltonian we use to reduce the cost as well as the automatic code generation process we used to derive and verify the cost scaling of the different terms. Overall, we find that our modifications have little impact on the method’s accuracy, which remains competitive with singles and doubles equation-of-motion coupled cluster.

I. INTRODUCTION

Although mean field methods like Hartree-Fock (HF) theory often succeed in making qualitatively correct predictions about how electrons distribute themselves within a molecule, making quantitative energetic predictions at the precision necessary to aid in designing and interpreting experiments usually requires grappling with the finer-grained wave function details that arise from electron correlation. In many contexts, especially when considering ground states in closed-shell molecules, density functional theory (DFT) fills this role at a relatively low computational expense. However, even in these DFT-friendly systems, there are areas – such as the treatment of weak intermolecular interactions¹ – where more expensive wave-function-based methods remain essential to, for example, help choose which empirical functional to trust. In electronically excited states, open-shell character is the norm, and in practice DFT faces serious challenges and is less predictive than in ground states. These challenges include both the inability of time-dependent DFT (TD-DFT) to relax the shapes of orbitals not directly involved in the excitation^{2–4} and the tendency of self-consistent DFT, as used for example in the restricted open-shell Kohn Sham (ROKS)^{5,6} method, to overdelocalize^{7,8} unpaired electrons or holes. Although the latter issue can be mitigated by using hybrid and range-separated functionals,⁹ it nonetheless persists.¹⁰ If wave-function-based methods are to help make up for DFT’s difficulties in this area, it is highly desirable that they overcome these challenges while retaining electron correlation corrections that are as computationally affordable as possible. In this study, we take a step in this direction by reformulating a second-order perturbative correction to excited state mean field (ESMF) theory^{10–12} so that its asymptotic cost scaling can reach parity with its ground state counterpart.

In the world of closed-shell ground states, the simplest and usually the most affordable approach to electron correlation aside from DFT is second-order Møller-Plesset perturbation

theory (MP2).¹³ In a canonical implementation, the asymptotic scaling of this method is $N_o^2 N_v^3$, where N_o and N_v denote the number of occupied and virtual orbitals in the HF reference, respectively.¹⁴ Note that, for simplicity, we will throughout this paper consider N_v to be interchangeable with N , the total number of molecular orbitals, when discussing asymptotic scaling. Although significantly higher than the cost scaling of many widely used density functionals, the cost of MP2 is significantly lower than the sixth-order cost of coupled cluster theory with singles and doubles (CCSD), positioning it as the least expensive wave-function-based ground state correlation method in wide use. The excited-state-specific ESMP2 theory¹¹ that we focus on in this study was designed to closely mirror MP2 theory, correcting ESMF in the same way that MP2 corrects HF, achieving rigorous size intensivity, and working in an uncontracted first order interacting space. Unfortunately, the fact that the ESMF reference already contains single excitations means that this interacting space now includes both the doubles and triples excitations. Acting the zeroth order Hamiltonian in this space thus involves contracting a two-index Fock operator with a six-index amplitude tensor, leading to seventh order scaling with the system size and a theory that is decidedly less practical than the ground state theory that it seeks to mimic.

To overcome this difficulty, we exploit the fact that a wave function that is a linear combination of singles excitations, such as configuration interaction singles (CIS), can be written as a sum of just N_o configuration state functions (CSFs) under a particular occupied-occupied and virtual-virtual rotation of the orbital basis. Working in this basis — which for CIS itself is the natural transition orbital basis¹⁵ but for ESMF will be slightly different due to its excited-state-specific orbital relaxations — the coulomb operator no longer connects the singly excited reference function to the whole triples space. Separating the triples in to those that connect with the reference and those that do not, one expects the unconnected triples (which are by far the larger group) to be less important, and so a more aggressive approximation of the zeroth order Hamiltonian in that space is somewhat justified. In particular, we will approximate the Fock operator in the unconnected space by its

^{a)}Electronic mail: eneuscamman@berkeley.edu

diagonal (note that, unlike for a HF reference, the Fock operator derived from the ESMF one-body density matrix is not diagonal) at which point the unconnected triples no longer contribute to the theory at all, as they have no direct connection to the reference through the coulomb operator and no connection to the first order wave function through the zeroth order Hamiltonian. As we will discuss, this step immediately drops the scaling to sixth order. To drop the scaling further, we note that, in the vast majority of low-lying excitations in weakly correlated molecules, only a small number out of the N_o singly excited CSFs in the ESMF reference are expected to have large coefficients. By extending the diagonal approximation of the zeroth order Hamiltonian into the space of all triples that only connect to small parts of the reference, a reduction to $N_o^2 N_v^3$ cost scaling is achieved. Again, as these triples are less important, this approximation is not expected to make much difference, and indeed this expectation is confirmed by a comparison to results from the seventh-order parent method. Thus, by working in a particular orbital basis and slightly modifying the zeroth order Hamiltonian, the cost scaling of ESMP2 can be brought in line with that of MP2, even if the prefactor remains higher due to the off-diagonal zeroth order Hamiltonian and thus a need to iteratively solve a linear equation.

Although ESMP2, in either its original or its more efficient form, is similar to a number of other excited state perturbation theories, it also possesses important differences. When compared to CIS(D), which uses the HF orbitals and derives its triples amplitudes from the ground state MP2 doubles,¹⁶ ESMP2 is instead wholly excited-state-specific: the orbitals are relaxed variationally for the excited state at the ESMF level, and the triples are derived via the excited state's first order wave function equation. In comparison to the recently-introduced driven similarity renormalization group VCIS-DSRG-PT2 approach,¹⁷ ESMP2 again enjoys orbitals that are relaxed for the excited state, and it does not require the choice of an active space, making it easier to apply in a black-box manner. Finally, in contrast with complete active space second order perturbation theory (CASPT2),^{18,19} N-electron valence perturbation theory (NEVPT2),²⁰ and VCIS-DSRG-PT2, ESMP2 sticks to an uncontracted and thus orthonormal first order interacting space, which circumvents the need to address the potential for linear dependencies. That said, ESMP2 has much in common with CASPT2, and as we will see in the results, often hews rather closely to CASPT2 when it comes to predicting excitation energies. Again, ESMP2 achieves this without using an active space, which offers significant simplicity at the cost of being inappropriate for strongly correlated systems.

This paper is organized as follows. We begin by discussing the ESMF reference and how it can be simplified by working in a particular orbital basis, after which we discuss the first order wave function and the newly-modified zeroth order Hamiltonian. We then briefly discuss the automated approach we employ for term derivation and code generation, which allows us to make a detailed investigation of each term's scaling, the outcomes of which we present in the first subsection of the results. We then delve into the method's accuracy, first in a

set of small molecules that are mostly single-CSF in character and then in a collection of ring excitations, in which multi-CSF character is more prevalent. We end our results section with an explicit test of size intensivity before concluding with a summary and a brief discussion of possible future directions.

II. THEORY

A. Zeroth Order Wave Function

To simplify our implementation, we have chosen to work with a slightly simplified version of the ESMF ansatz

$$|\Psi_0\rangle = e^{\hat{X}} \sum_{ia} C_{ia} (\hat{a}_{a\uparrow}^+ \hat{a}_{i\uparrow} \pm \hat{a}_{a\downarrow}^+ \hat{a}_{i\downarrow}) |\Phi\rangle \quad (1)$$

in which we have set the coefficient on the un-excited closed-shell reference determinant $|\Phi\rangle$ to zero. This simplification avoids a significant number of terms in the perturbation theory, but it does mean that we are assuming that the closed shell determinant is unimportant in the excited state, which is not universally true. Here the \pm sign is plus (minus) for singlet (triplet) states, C is the matrix of single-excitation configuration interaction (CI) coefficients, \hat{X} is an anti-Hermitian one-electron operator responsible for excited-state-specific orbital relaxations, and we adopt the convention of referring to occupied and unoccupied (virtual) orbitals in $|\Phi\rangle$ by the indices i, j, k, l and a, b, c, d , respectively. After relaxing \hat{X} and C to find the energy stationary point corresponding to the excited state in question (which may for example proceed by guessing the CIS wave function and applying a generalized variational principle¹²), we take a singular value decomposition of the rectangular matrix C

$$C = U \Lambda V^+ \quad (2)$$

where, if we assume that there are more virtual than occupied orbitals, Λ is the $N_o \times N_o$ diagonal matrix of singular values. Now, note that the Hamiltonian can be transformed into an orbital basis that eliminates U and V and thus renders the reference wave function in a particularly simple form.

$$\hat{H}^{\text{HF}} \rightarrow e^{-\hat{Z}} e^{-\hat{Y}} e^{-\hat{X}} \hat{H}^{\text{HF}} e^{\hat{X}} e^{\hat{Y}} e^{\hat{Z}} \quad (3)$$

Here we have started in the HF orbital basis (as indicated by the Hamiltonian \hat{H}^{HF}), rotated via \hat{X} into the ESMF orbital basis, and then rotated via the one-electron anti-Hermitian operators \hat{Y} and \hat{Z} , which perform occupied-occupied and virtual-virtual rotations, respectively. The \hat{Y} rotation can be chosen so as to eliminate U , and likewise the \hat{Z} rotation can be used to eliminate V , leaving us with a greatly simplified CI expansion

$$|\Psi_0\rangle \rightarrow \sum_i \Lambda_{ii} (\hat{\sigma}_{i\uparrow}^+ \hat{\tau}_{i\uparrow} \pm \hat{\sigma}_{i\downarrow}^+ \hat{\tau}_{i\downarrow}) |\Phi\rangle \quad (4)$$

involving a sum over the singular values of C . The corresponding virtual-orbital creation operators $\hat{\sigma}^+$ and occupied-orbital destruction operators $\hat{\tau}$ now come in pairs, one for each occupied orbital. We refer to each of these pairs as a transition

orbital pair (TOP), and note that, if the optimal ESMF orbitals were the same as the RHF orbitals, the TOPs would be equivalent to the natural transition orbital (NTO) pairs.¹⁵ It is important to emphasize that Eqs. (1) and (4) refer to exactly the same zeroth order wave function, they simply express it in different orbital bases. We now turn to the definition of our first order wave function, where the TOP basis will allow for useful groupings of the triples excitations into separate categories that we will exploit in order to achieve a lower asymptotic cost scaling.

B. First Order Wave Function

To begin, let us specify the language we will use for describing excitations as well as the the different orbital labels that we employ when working in the TOP orbital basis. First, throughout this paper, we will refer to excitation levels relative to the closed shell. In this language, our reference is a superposition of single excitations, and our first-order interacting space consists of double and triple excitations. As for how we label orbitals, let us adopt an orbital ordering in which the spatial orbitals are numbered 1 through N . In addition to the occupied orbitals with destruction operators \hat{t}_i (with i allowed to range from 1 through N_o) and the corresponding TOP virtual orbitals whose creation operators are $\hat{\sigma}_a^+$ (with a allowed to range from $N_o + 1$ through $2N_o$), there are additional virtual orbitals (AVOs), whose creation operators we will denote by \hat{v}_a^+ (with a allowed to range from $2N_o + 1$ through N). When necessary, we will denote virtual orbitals that may be either TOP virtuals or AVOs using the creation operators \hat{w}_a^+ , where a can range from $N_o + 1$ through N . Finally, when we denote a TOP virtual orbital using an occupied index, as for example in the operator $\hat{\sigma}_{i\uparrow}^+$ in Eq. (4), this implies the TOP virtual orbital with index $a = i + N_o$ that is the partner of the i th occupied orbital in the TOP orbital basis representation of $|\Psi_0\rangle$.

With these orbital definitions in hand and working in the TOP orbital basis, we now point out that while the Hamiltonian, through its two-electron part, can connect the singly-excited wave function $|\Psi_0\rangle$ to the full space of doubly excited determinants, it only connects $|\Psi_0\rangle$ to a subset of the triply excited determinants. In particular, the matrix element

$$H_{ijk}^{abc} = \langle \Psi_0 | \hat{t}_k^+ \hat{t}_j^+ \hat{t}_i^+ \hat{w}_a \hat{w}_b \hat{w}_c \hat{H} | \Psi_0 \rangle \quad (5)$$

will only be nonzero if there is at least one TOP amongst the occupied and virtual orbitals i, j, k, a, b, c . Put another way, this matrix element is zero if $d \neq l + N_o$ for all $d \in \{a, b, c\}$ and $l \in \{i, j, k\}$, as a nonzero element is only possible if one of the three excitations was already present in $|\Psi_0\rangle$, and $|\Psi_0\rangle$ only contains TOP excitations. In contrast, this matrix element can be nonzero if $d = l + N_o$ for at least one d, l pair from $d \in$

$\{a, b, c\}$ and $l \in \{i, j, k\}$. Thus, in our first order wave function

$$\begin{aligned} |\Psi_1\rangle = & \sum_{ijab} T_{ij}^{ab} \hat{w}_{a\uparrow}^+ \hat{w}_{b\uparrow}^+ \hat{t}_{j\uparrow} \hat{t}_{i\uparrow} |\Phi\rangle \\ & + \sum_{ijab} T_{ij}^{ab} \hat{w}_{a\downarrow}^+ \hat{w}_{b\downarrow}^+ \hat{t}_{j\downarrow} \hat{t}_{i\downarrow} |\Phi\rangle \\ & + \sum_{ijab} S_{ij}^{ab} \hat{w}_{a\uparrow}^+ \hat{w}_{b\downarrow}^+ \hat{t}_{j\downarrow} \hat{t}_{i\uparrow} |\Phi\rangle \\ & + \sum_{ijkabc} T_{ijk}^{abc} \hat{w}_{a\uparrow}^+ \hat{w}_{b\uparrow}^+ \hat{w}_{c\uparrow}^+ \hat{t}_{k\uparrow} \hat{t}_{j\uparrow} \hat{t}_{i\uparrow} |\Phi\rangle \\ & + \sum_{ijkabc} T_{ijk}^{abc} \hat{w}_{a\downarrow}^+ \hat{w}_{b\downarrow}^+ \hat{w}_{c\downarrow}^+ \hat{t}_{k\downarrow} \hat{t}_{j\downarrow} \hat{t}_{i\downarrow} |\Phi\rangle \\ & + \sum_{ijkabc} S_{ijk}^{abc} \hat{w}_{a\uparrow}^+ \hat{w}_{b\downarrow}^+ \hat{w}_{c\downarrow}^+ \hat{t}_{k\downarrow} \hat{t}_{j\downarrow} \hat{t}_{i\uparrow} |\Phi\rangle \\ & + \sum_{ijkabc} S_{ijk}^{abc} \hat{w}_{a\downarrow}^+ \hat{w}_{b\uparrow}^+ \hat{w}_{c\uparrow}^+ \hat{t}_{k\uparrow} \hat{t}_{j\uparrow} \hat{t}_{i\downarrow} |\Phi\rangle \end{aligned} \quad (6)$$

we set to zero the values of all same-spin (T_{ijk}^{abc}) and mixed-spin (S_{ijk}^{abc}) triples coefficients whose indices do not contain at least one TOP. As we will choose our zeroth order Hamiltonian to be diagonal in the space of triples excitations that contain no TOPs (which we define as the N-triples space), setting these coefficients to zero is not an approximation, but merely the natural consequence of their Eq. (5) matrix elements being zero and \hat{H}_0 not connecting them to any other parts of $|\Psi_1\rangle$. Instead, the new approximation, and the key difference from our previous N^7 -scaling excited-state-specific perturbation theory,¹¹ comes in the definition of \hat{H}_0 , to which we now turn our attention.

C. Zeroth Order Hamiltonian

In our previous N^7 -scaling version of the theory, we chose the zeroth order Hamiltonian to have the following form.

$$\hat{H}_0 = \hat{R}(\hat{F} - \hat{H})\hat{R} + \hat{P}\hat{H}\hat{P} + \hat{Q}\hat{F}\hat{Q} \quad (7)$$

Here, we will retain this form, but make some modifications in the triples space to improve efficiency. As before, we take \hat{F} to be the Fock operator constructed from the one-body density matrix of $|\Psi_0\rangle$, $\hat{R} = |\Psi_0\rangle \langle \Psi_0|$ to be the projector on to the zeroth order wave function, \hat{P} to be the projector on to the span of the closed shell determinant $|\Phi\rangle$ and all singly excited determinants, and $\hat{Q} = 1 - \hat{P}$. The difference between the present theory and our previous approach is that, in the present theory, we work in the TOP orbital basis and modify the $\hat{Q}\hat{F}\hat{Q}$ term so that it is diagonal in some parts of the triples space. To see how, let us first organize the triply excited determinants into three groups: the N-triples whose six indices i, j, k, a, b, c do not contain any TOPs, the L-triples that contain at least one TOP whose singular value from Eq. (4) is large (above a threshold η), and the S-triples that contain at least one TOP but whose TOPs all have small singular values (below η). With the triples organized into these three groups, we

make the modification

$$\begin{aligned} \hat{Q}\hat{F}\hat{Q} \rightarrow & (\hat{Q}_D + \hat{Q}_L)\hat{F}(\hat{Q}_D + \hat{Q}_L) \\ & + (\hat{Q}_S + \hat{Q}_N)\hat{F}^{(\text{diag})}(\hat{Q}_S + \hat{Q}_N) \end{aligned} \quad (8)$$

in which $\hat{F}^{(\text{diag})}$ is the Fock operator with its off-diagonal terms set to zero and \hat{Q}_D , \hat{Q}_L , \hat{Q}_S , and \hat{Q}_N project on to the doubles, the L-triples, the S-triples, and the N-triples, respectively. As shown in Figure 1, we are making \hat{H}_0 diagonal for the presumably less important S-triples and N-triples, whereas our previous approach left it off-diagonal for all triples.

How much efficiency is gained by this approach depends on how one chooses to divide the TOP-containing triples between the large and small L-triples and S-triples spaces. In the $\eta = 0$ extreme, in which all the TOP-containing triples are placed in the L-triples space, the cost of forming the right-hand-side of and solving the usual Rayleigh-Schrödinger linear equation for $|\Psi_1\rangle$ grows as N^6 . The reduction from the N^7 scaling of our previous approach comes from eliminating the N-triples, which as discussed in Section II B have no Eq. (5) matrix elements and thus can only contribute to the theory by coupling through \hat{H}_0 to other parts of $|\Psi_1\rangle$, which is prevented by our modification in Eq. (8). In the other extreme, when only triples that contain the TOP with the largest singular value are placed in the L-triples space and all other TOP-containing triples are placed in the S-triples space, the cost of setting up and solving the linear equation for $|\Psi_1\rangle$ grows as only N^5 . Note that, as we explain in Section III B, we have explicitly verified these scalings (the lower of which is actually $N_o^2 N_v^3$) by log-log regressions on the floating-point operation counts of each individual term entering in to the setup and iterative solution of the linear equation.

To put these extremes in to perspective, we note that for a size-intensive excitation, by which we mean one whose spatial extent does not grow indefinitely as the system is enlarged, the number of non-zero singular values in Eq. (4) will be constant with system size in the large system limit. This implies that for size-intensive excitations, setting η to a small but non-zero threshold will result in both a size-intensive excitation energy (a property we verify explicitly below) and N^5 scaling. Note that this efficiency gain is *not* due to assuming anything about the locality of electron correlation (which if exploited as in some ground state methods²¹ could perhaps further lower the method's scaling) but instead comes from the natural tendency of molecular excitations to be localized. Of course, in practice, the length scale needed to see this benefit may be much larger than the simulation in a particular system, so let us make a more concrete statement about the scaling. If one limits $|\Psi_0\rangle$ to have only N_{TOP} nonzero singular values regardless of the system size, then the method has an N^5 scaling. The obvious practical case where this approach should be useful is for excitations that are dominated by a single configuration state function (CSF), and thus for which only one singular value is nonzero anyways.

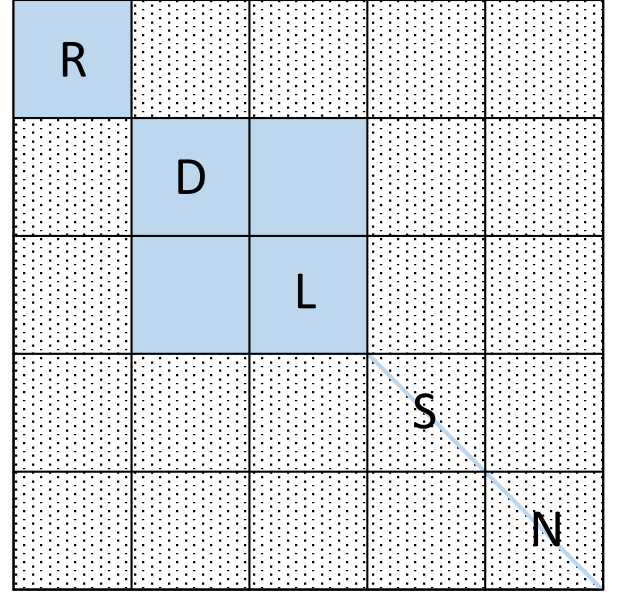


FIG. 1: Block structure of the zeroth order Hamiltonian. The matrix is zero in the dotted regions and non-zero in the blue regions, including on the diagonal of blocks S and N. The blocks are labeled as R for $|\Psi_0\rangle$, D for double excitations, L for triple excitations containing at least one TOP with a large singular value, S for all other triple excitations containing at least one TOP, and N for the triple excitations that contain no TOPs. Note that no singly excited states are included in our first-order interacting space, on the theory that the effects of these states have already been included by the variational optimization of the reference.

D. Automated Implementation

For the construction and solution of the linear equation for $|\Psi_1\rangle$, we have written a simple for-loop generator. The approach is to start with a symbolic representation of the for-loops belonging to each orbital index, and then to use Wick's theorem to derive the different contraction schemes that connect indices and thus eliminate for-loops via the resulting Kronecker delta functions. This entire process is automated and includes the detailed logic needed to a) identify which triples reside in the L-triples space and thus must be included in the iterative solution of the linear equation (triples in the S and N spaces are not part of the iterative solver, as their part of the linear equation is diagonal and can be inverted directly) and b) avoid double counting redundant terms, such as T_{ijk}^{abc} and T_{jik}^{bac} . Of course, the result is a code build of “dumb” loops, which will not be cache-optimal, but does provide us with a correct reference implementation to start from. Further, it allows us to automatically implement careful operation counting, such that each contraction can have its cost scaling analyzed independently. Having thus identified the most expensive term (which turns out to be a contraction between the mixed-spin-L-triples and the Fock operator) we have verified that by hand-coding this term in terms of dense linear algebra, the cost can be re-

duced by more than an order of magnitude. In future, we will work to convert all other contractions whose cost is not trivial into dense linear algebra. In the present study, however, our focus is not on a production-level code, but instead on completing a detailed analysis of the cost-scaling as well as the accuracy of the new N^5 approach.

For an example of how the code generation works, consider how the Fock operator might map double excitation coefficients to L-triples excitation coefficients in the case where all orbitals are spin up. The corresponding tensor contractions come from the different ways of contracting the indices in

$$\sum_{pq} \sum_{i'j'a'b'} F_{pq} T_{i'j'}^{a'b'} \langle \Phi | \hat{\tau}_k^+ \hat{\tau}_i^+ \hat{\tau}_j^+ \hat{w}_b \hat{w}_a \hat{\sigma}_c \hat{a}_p^+ \hat{a}_q \hat{w}_a^+ \hat{w}_b^+ \hat{\tau}_{j'} \hat{\tau}_{i'} | \Phi \rangle, \quad (9)$$

where the L-triple's indices are i, j, k, a, b, c and we assume, without loss of generality, that c and k form a TOP such that $c = k + N_o$ (at least one TOP must be present as this is an L-triple). The automatically generated code for one of the contractions resulting from Eq. (9) is seen in Figure 2, where we see explicitly in the second line of code the simplification and lower scaling that comes if we fix the number N_{TOP} of large TOPs. This particular term has $N_o^2 N_v^2$ scaling if the number of large-singular-value TOPs is fixed, or $N_o^3 N_v^2$ if it grows with system size (e.g. if all TOPs are considered large). Across all the different pieces needed to construct the linear equation's right-hand-side and to operate by \hat{H}_0 , the automated generator found 185 contractions with non-zero contributions. When N_{TOP} is set to one, only 18 of the contractions involving triples showed fifth-order cost-scaling, and only 9 of those showed the most expensive $N_o^2 N_v^3$ scaling, suggesting that converting the worst terms to hand-coded dense linear algebra (i.e. BLAS) should be feasible in future work. See section III B below for a more detailed cost scaling analysis.

III. RESULTS

A. Computational Details

For ESMP2, we used the iterative conjugate-gradient algorithm to solve the linear equation for $|\Psi_1\rangle$. The EOM-CCSD and δ -CR-EOM-CC(2,3)^{22–25} calculations were performed with GAMESS,^{26,27} whereas CIS and TDDFT calculations were performed with QChem.²⁸ CASPT2 calculations for the ring excitations were performed with Molpro.^{29–31} Note that, although some CASPT2 calculations relied on state-averaged CASSCF reference functions, the CASPT2 calculations themselves were single-state. In the pyrrole molecule, CASSCF was performed with a (10o,6e) active space, in which an equal-weight 4-state state-average was employed, with 2, 1, and 1 states from the A_1 , A_2 , and B_2 representations, respectively. Note that pyrrole's 2^1A_1 excitation was not stable in CASPT2 without a level shift, and so in this molecule a level shift of 0.2 E_h was used for all states. In the rest of the ring excitations, CASPT2 was stable without a level shift, and so no shift was used in other molecules. For pyridine, CASSCF em-

```
for ( int k = 0; k < nocc; k++ ) {
  if ( k >= ntop ) continue;
  const int c = (k+nocc);
  for ( int i = 0; i < nocc; i++ ) {
    if ( i == k ) continue;
    for ( int j = i+1; j < nocc; j++ ) {
      if ( j == k ) continue;
      for ( int a = nocc; a < norb; a++ ) {
        if ( a == c ) continue;
        if ( a == i + nocc && i <= k ) continue;
        if ( a == j + nocc && j <= k ) continue;
        for ( int b = a+1; b < norb; b++ ) {
          if ( b == c ) continue;
          if ( b == i + nocc && i <= k ) continue;
          if ( b == j + nocc && j <= k ) continue;
          const int ip = i;
          if ( ip >= nocc ) continue;
          const int jp = j;
          if ( jp < ip+1 ) continue;
          if ( jp >= nocc ) continue;
          const int ap = a;
          if ( ap < nocc ) continue;
          const int bp = b;
          if ( bp < ap+1 ) continue;
          const int p = c;
          const int q = k;
          out(k,i,j,a,b) += fm(p,q) * in(ip,jp,ap,bp);
        }
      }
    }
  }
}
```

FIG. 2: The generated code for the $\delta_{aa'}\delta_{bb'}\delta_{ii'}\delta_{jj'}\delta_{kk'}\delta_{cp}$ contraction resulting from Eq. (9). Note the second line, where the scaling is explicitly reduced if the number N_{TOP} of TOPs that are considered large does not grow with system size.

ployed an (8o,10e) active space and four separate state averaging calculations, one in each representation of its C_{2v} point group. No level shift was necessary for stability in pyridine, but each of these four calculations used an equal-weight 3-state state average, which was necessitated by the fact that at the CASSCF level the 1^1B_2 and 2^1B_2 states come first and third in the energy ordering of the 1^1B_2 states. For benzene, CASSCF employed a (6o,6e) active space for an equal-weight 6-state state-average with two states each in the A_g , B_{1u} , and B_{2u} representations (the computational point group was D_{2h}). Finally, for pyrimidine, CASSCF employed an (8o,10e) active space. As all the states investigated in pyrimidine are ground states within their own symmetries, state averaging was not used in this case.

B. Cost Scaling Analysis

Before looking at the energetic accuracy of reduced-scaling ESMP2, let us first inspect how the different components scale with the number of occupied and virtual orbitals. Using our automatic code generator, we have inserted operation counting into all of the terms, allowing for a contraction-by-contraction scaling analysis. For each contraction, we measured occupied scaling by fixing the number of virtual orbitals at 100 and varying the number of occupied orbitals between 30 and 50, after which we perform a log-log linear regression on each contraction's operation count. Similarly, for scaling with virtual orbitals, we have fixed the number of occupied orbitals at 30 and varied the number of virtuals between 50 and 100, again feeding the information into log-log lin-

TABLE I: Scaling data for ESMP2-TOP(1), in which only one TOP is treated as large and which is thus most appropriate when the reference is dominated by a single CSF. For the different parts of the PT2 linear equation’s right-hand side (RHS) and linear transformation, we report how many of that part’s contractions fall in to the different asymptotic scaling categories.

	N^3	$N_o^3 N_v$	$N_o^2 N_v^2$	$N_o^3 N_v^2$	$N_o^2 N_v^3$
T_{ij}^{ab} (RHS)	4	12	6	0	0
S_{ij}^{ab} (RHS)	2	6	3	0	0
T_{ijk}^{abc} (RHS)	16	0	4	0	0
S_{ijk}^{abc} (RHS)	3	0	5	0	0
$T_{ij}^{ab} \leftrightarrow T_{ij}^{ab}$	0	0	1	2	2
$S_{ij}^{ab} \leftrightarrow S_{ij}^{ab}$	0	0	1	2	2
$T_{ijk}^{abc} \leftrightarrow T_{ijk}^{abc}$	0	0	3	4	4
$S_{ijk}^{abc} \leftrightarrow S_{ijk}^{abc}$	0	0	2	5	5
$T_{ijk}^{abc} \leftrightarrow T_{ij}^{ab}$	0	0	18	0	0
$S_{ijk}^{abc} \leftrightarrow S_{ij}^{ab}$	0	0	8	0	0
$S_{ijk}^{abc} \leftrightarrow T_{ij}^{ab}$	0	0	2	0	0

ear regressions. We present two sets of scaling data, representing the two cost extremes that one can get from the new approach. First, Table I shows the scaling data for ESMP2-TOP(1), in which only one TOP is considered large. Second, Table II shows the scaling data for ESMP2-TOP(all), in which all TOPs are considered large and the S-triples space is thus empty.

This detailed scaling analysis reveals that the worst-scaling terms all reside in the linear transformation part of solving the PT2 linear equation, which is to say evaluating the action of H_0 on a vector in the first-order interacting space as required in each iteration of the conjugate gradient algorithm we use to solve the linear equation. These terms are fifth and sixth order in the system size for ESMP2-TOP(1) and ESMP2-TOP(all), respectively, showing that it is indeed possible to improve over the seventh order scaling of the original formulation of ESMP2. Of course, prefactors matter, and the fact that ESMP2-TOP(1) carries 13 terms with $N_o^2 N_v^3$ scaling means that, for small systems, it will almost certainly be slower than EOM-CCSD despite its lower scaling, as EOM-CCSD has a smaller number of N^5 and N^6 terms. The scaling does guarantee, though, that ESMP2-TOP(1) will be faster in larger systems. We now turn our attention to the question of whether energetic accuracy is maintained when we aggressively limit the number of TOPs that are considered large.

C. Small Molecule Testing

Let us begin by testing the fifth order method on the same set of small molecules and two charge transfer (CT) examples that were studied recently with the original seventh order in-

TABLE II: Scaling data for ESMP2-TOP(all), in which all TOPs are treated as large. For the different parts of the PT2 linear equation’s right-hand side (RHS) and linear transformation, we report how many of that part’s contractions fall in to the different asymptotic scaling categories. We omit the RHS doubles terms and the doubles-only parts ($T_{ij}^{ab} \leftrightarrow T_{ij}^{ab}$ and $S_{ij}^{ab} \leftrightarrow S_{ij}^{ab}$) of the linear transformation, as their scaling is the same as in Table I. Note that in cases where the log-log scaling regression exponents for occupied or virtual orbitals were significantly fractional (i.e. differed from integers by more than 0.3) we took the conservative approach of transferring enough fractional exponent from occupied to virtual in order to move the virtual exponent up to the next integer, and then rounded what remained of the fractional occupied exponent up or down if it was above or below 0.3. For example, $N_o^{2.6} N_v^{2.5}$ is converted to $N_o^2 N_v^3$, while $N_o^{2.99} N_v^{1.35}$ is converted to $N_o^3 N_v^2$. Note that, although this conservative rounding may slightly rearrange the contractions among the N^4 and N^5 categories, we have explicitly verified (by inspecting the code) that each of the N^6 contractions has the asymptotic scaling reported here.

	N^4	N_o^5	$N_o^4 N_v$	$N_o^3 N_v^2$	$N_o^2 N_v^3$	$N_o^4 N_v^2$	$N_o^3 N_v^3$
T_{ijk}^{abc} (RHS)	16	0	0	4	0	0	0
S_{ijk}^{abc} (RHS)	3	0	0	5	0	0	0
$T_{ijk}^{abc} \leftrightarrow T_{ijk}^{abc}$	0	25	8	13	10	7	4
$S_{ijk}^{abc} \leftrightarrow S_{ijk}^{abc}$	0	2	5	6	1	5	5
$T_{ijk}^{abc} \leftrightarrow T_{ij}^{ab}$	0	10	10	20	10	0	0
$S_{ijk}^{abc} \leftrightarrow S_{ij}^{ab}$	0	0	0	8	0	0	0
$S_{ijk}^{abc} \leftrightarrow T_{ij}^{ab}$	0	0	4	2	2	0	0

carnation of ESMP2. To make the comparison direct, we use the same cc-pVDZ basis and the same molecular geometries as in the previous study.¹² Here, we restrict the L-triples space as much as possible by treating only the dominant TOP (or, in the case of N_2 , the pair of equal-weight dominant TOPs) as large, relegating triples that do not contain the dominant TOP to the S-triples space with its diagonally-approximated zeroth order Hamiltonian. In Table III, we see that for this set of small molecules, this $N_o^2 N_v^3$ -scaling variant of ESMP2 is, like its seventh order predecessor, competitive in accuracy with EOM-CCSD. Thus, by working with excited-state-specific orbitals from the ESMF reference and an excited-state-specific correlation treatment from ESMP2, it is possible, at least in these test systems, to achieve EOM-CCSD accuracies with a method that scales as the fifth order of the system size. As with the original formulation of ESMP2, we find it especially encouraging that the method is equally accurate for CT and non-CT states, as practical uses of CT in biological and energy-related chemistry often involve large system sizes where lower-scaling methods are essential.

Interestingly, the results here are barely changed compared to the results from the previous seventh order method, which displayed mean absolute errors of 0.13 eV and 0.12 eV for

TABLE III: For the lowest singlet excitations in several small molecules, as well as for two simple CT excitations, we report the reference δ -CR-EOM-CC(2,3) excitation energy in eV, as well as other methods’ errors relative to the reference. All calculations are in the cc-pVDZ basis. Only the dominant TOPs were considered large in ESMP2, meaning one TOP in all cases except N_2 , where by symmetry there are two dominant TOPs with equal weights. Below each method, we report the canonical cost scaling with respect to system size. At bottom, we report mean and maximum absolute (i.e. unsigned) deviations from the reference both with and without the CT systems included, as well as the number of deviations larger than 0.3 eV.

	δ -CR-EOM-CC(2,3) $O(N^7)$	CIS $O(N^4)$	TDDFT/B3LYP $O(N^4)$	TDDFT/ ω B97X $O(N^4)$	EOM-CCSD $O(N^6)$	ESMP2 $O(N^5)$
Acetaldehyde $1^1A''$	4.36	0.71	0.09	0.14	0.21	0.16
Ammonia 2^1A_1	7.57	0.95	-0.52	-0.07	0.05	0.01
Carbon Monoxide $1^1\Pi$	8.76	0.61	0.16	0.31	0.30	-0.09
Cyclopropene 2^1B_2	7.97	0.57	-0.83	-0.33	-0.08	-0.07
Diazomethane 1^1A_2	3.01	0.38	0.05	0.09	0.45	-0.00
Dinitrogen $1\Pi_g$	10.36	-1.31	-0.03	0.00	0.44	0.09
Ethylene 1^1B_3	8.80	-0.25	0.11	0.10	0.19	-0.30
Formaldehyde 1^1A_2	4.08	0.63	0.07	0.10	0.19	0.15
Formamide $2^1A''$	5.86	0.88	0.04	0.11	0.21	0.15
Hydrogen Sulfide 2^1B_2	7.05	0.58	-0.27	0.20	0.11	-0.07
Ketene 1^1A_2	3.78	0.70	0.22	0.31	0.36	-0.01
Methanimine $1^1A''$	5.35	0.66	0.00	0.11	0.22	-0.00
Nitrosomethane $1^1A''$	1.85	0.27	0.13	0.12	0.25	0.17
Streptocyanine Cation 1^1B_2	7.53	1.55	1.08	1.07	0.28	-0.40
Thioformaldehyde 1^1A_2	2.18	0.58	0.13	0.17	0.24	-0.08
Water 1^1B_2	8.30	1.02	-0.57	-0.22	-0.01	0.06
Ammonia \rightarrow Difluorine 2^1A_1	9.27	2.38	-6.91	-2.69	0.51	-0.26
Dinitrogen \rightarrow Methylene 1^1B_2	15.49	1.66	-6.58	-1.79	0.06	0.15
Mean Abs. Dev. (with CT)		0.87	0.99	0.44	0.23	0.12
Max Abs. Dev. (with CT)		2.38	6.91	2.69	0.51	0.40
Mean Abs. Dev. (without CT)		0.73	0.27	0.22	0.22	0.11
Max Abs. Dev. (without CT)		1.55	1.08	1.07	0.45	0.40
Deviations above 0.3 eV		16	6	6	4	1

the full set and the non-CT subset, respectively.¹² This finding suggests that the basic idea here is sound: using a diagonal approximation to H_0 in the space of less-important triples does not have a significant effect on the accuracy. Note that we have tested whether having any off-diagonal H_0 character in the triples manifold is necessary by testing what happens if no TOPs are treated as large. In that case, we find that accuracy suffers significantly, suggesting that, for the triples that connect directly via the coulomb operator to the large parts of the zeroth order reference, the fact that the Fock operator is not diagonal is significant. Thus, it appears that we get away with the reduction in scaling not because the off-diagonal parts of the Fock operator are unimportant, but because their effects are small for the triples that do not connect to the reference or that only connect to small components (TOPs with small weights) of the reference.

D. Ring Excitations

We now turn to a set of low-lying excitations in aromatic ring systems, where it is common to see excited states in which more than one TOP has a large weight. For these systems (whose geometries have been taken from the cc-pVDZ MP2 entries in the CCCBDB NIST database³²) we have defined large TOPs as those whose singular values are above 0.1, resulting in two or fewer large TOPs in each excitation and thus a method that remains at the fifth-order end of the continuum between ESMP2-TOP(1) and ESMP2-TOP(all). Unlike the small molecules of the previous section, some of these ring excitations have at least a modest (although not dominant) degree of doubly excited character. As CASPT2 is often used to address double excitations, we have also included a comparison against its results in the table, although we stress that δ -CR-EOM-CC(2,3) is the better reference in these states thanks to its ability to handle double excitations and its higher-order treatment of electron correlation. This comparison makes clear that, at least on average, ESMP2 is more simi-

TABLE IV: Excitation energies (eV) for small ring systems in the cc-pVDZ basis. For the δ -CR-EOM-CC(2,3) reference, we report the excitation energy, while for other methods we report deviations from the reference. ESMP2 treated TOPs with singular values above 0.1 as large, which led to two or fewer large TOPs in all states included here. A diagonal H_0 was used in the space of triples that do not contain any large TOPs. At the bottom, we report mean and maximum absolute deviations from the reference, the number of these deviations that were larger than 0.3 eV, and the mean absolute deviation from CASPT2.

State	δ -CR-EOM-CC(2,3)	CIS	TDDFT/B3LYP	TDDFT/ ω B97X	EOM-CCSD	CASPT2	ESMP2
Pyrrole 2^1A_1	6.15	1.60	0.45	0.84	0.51	-0.18*	-0.90
Pyrrole 1^1A_2	6.39	0.86	-0.48	0.70	0.36	0.10	0.09
Pyrrole 1^1B_2	6.56	0.37	0.01	0.10	0.47	0.38	-0.21
Pyridine 1^1B_1	4.84	1.33	-0.01	0.36	0.44	0.10	0.11
Pyridine 1^1B_2	4.76	1.44	0.75	0.83	0.52	0.07	-0.25
Pyridine 2^1B_2	6.51	2.05	0.86	1.05	0.45	0.29	0.11
Pyridine 1^1A_2	5.26	2.19	-0.16	0.33	0.44	-0.05	-0.05
Benzene 1^1B_{2u}	4.69	1.33	0.72	0.83	0.50	0.06	-0.71
Benzene 1^1B_{1u}	6.35	-0.08	-0.21	-0.06	0.42	-0.35	-0.26
Benzene 2^1B_{1u}	7.33	0.94	-0.14	-0.01	0.43	-0.69	-0.82
Pyrimidine 1^1B_1	4.50	1.40	-0.21	0.18	0.22	-0.32	-0.82
Pyrimidine 1^1B_2	5.23	1.28	0.52	0.61	0.28	-0.22	-0.28
Mean Abs. Dev. (MAD)		1.24	0.38	0.49	0.42	0.23	0.38
Max Abs. Dev.		2.19	0.86	1.05	0.52	0.69	0.90
Deviations above 0.3 eV		11	6	8	10	4	4
MAD vs CASPT2		1.30	0.44	0.59	0.49	0.00	0.28

*Level shift was necessary for convergence. See text.

TABLE V: Excitation energies (eV) for small ring systems in the cc-pVTZ basis. For the δ -CR-EOM-CC(2,3) reference, we report the excitation energy, while for other methods we report deviations from the reference. ESMP2 treated TOPs with singular values above 0.1 as large, which led to two or fewer large TOPs in all states included here. A diagonal H_0 was used in the space of triples that do not contain any large TOPs. At the bottom, we report mean and maximum absolute deviations from the reference and the number of these deviations that were larger than 0.3 eV.

State	δ -CR-EOM-CC(2,3)	EOM-CCSD	ESMP2
Pyrrole 2^1A_1	5.95	0.59	-0.89
Pyrrole 1^1A_2	5.93	0.41	0.13
Pyrrole 1^1B_2	6.25	0.15	-0.18
Pyridine 1^1B_1	4.69	0.52	0.15
Pyridine 1^1B_2	6.22	0.51	0.12
Pyridine 2^1B_2	4.61	0.60	-0.21
Pyridine 1^1A_2	5.14	0.51	-0.03
Benzene 1^1B_{2u}	4.55	0.58	-0.66
Benzene 1^1B_{1u}	7.01	0.51	-0.76
Benzene 2^1B_{1u}	6.06	0.48	-0.23
Pyrimidine 1^1B_1	4.14	0.54	-0.60
Pyrimidine 1^1B_2	4.82	0.62	-0.23
Mean Abs. Dev. (MAD)		0.51	0.35
Max Abs. Dev.		0.62	0.89
Deviations above 0.3 eV		11	4

lar to CASPT2 than to δ -CR-EOM-CC(2,3), which is perhaps not surprising given the fact that ESMP2 and CASPT2 approach these states via second order perturbation theory from a qualitatively correct reference, making them methodologically similar. Of course, the fact that ESMP2 need not specify an active space is a significant practical advantage.

Across the twelve ring excitations shown in Table IV, we

find that the differences between EOM-CCSD and ESMP2 are more significant than in the small-molecule excitations of the last section. While EOM-CCSD has a slightly higher mean absolute deviation from δ -CR-EOM-CC(2,3), its deviations are more regular than those of ESMP2. Indeed, in all twelve cases, EOM-CCSD predicts excitation energies to be between 0.2 and 0.55 eV higher than does δ -CR-EOM-

TABLE VI: Results for a few Rydberg states in neon, formaldehyde, and benzene. Molecular geometries were taken from the NIST CCCBDB database.³² All values are reported in eV.

State	Basis	ESMF	N5-ESMP2	Error
Neon (2s \rightarrow 3p)	cc-pVTZ	65.6781	64.6521	0.35 ^a
Formaldehyde 2 ¹ A ₁	d-aug-cc-pVTZ	7.0967	8.3287	0.23 ^b
Formaldehyde 3 ¹ A ₁	d-aug-cc-pVTZ	8.1856	9.3947	0.13 ^b
Benzene 1E _{2g}	aug-ANO1 ^c	6.7758	7.4583	-0.38 ^c
Benzene 2A _{1g}	aug-ANO1 ^c	6.7619	7.4557	-0.39 ^c
Benzene 1A _{2g}	aug-ANO1 ^c	6.8013	7.4856	-0.38 ^c

^a Compared to EOM-CCSD in the same basis.¹¹

^b Compared to the theoretical best estimate for these states.³³

^c Compared to CCSD calculations in the same basis set.³⁴

CC(2,3), whereas the span of ESMP2’s deviations is significantly larger at just over an eV. Table V shows that a similar story plays out for EOM-CCSD and ESMP2 in a triple-zeta basis, reassuring us that these tendencies are not specific to the double-zeta basis, on which we now focus our attention.

Notably, while Table IV’s ESMP2 results are within 0.3 eV of δ -CR-EOM-CC(2,3) for eight out of the twelve states, in the other four states — pyrrole 2¹A₁, benzene 1¹B_{2u}, benzene 2¹B_{1u}, and pyrimidine 1¹B₁ — its prediction is low by 0.7 eV or more. Two of these are errors likely due to doubly excited character, one an error related to intruder states issues, and one is not necessarily much of an error at all. Start with the 2¹A₁ state of pyrrole, where CASPT2 displays intruder-state behavior and is not stable without the application of a level shift. Given that the zeroth order Hamiltonians are similar, and that the CASSCF reference used by CASPT2 should be a better starting point than ESMF, ESMP2’s difficulty in this state is likely related to these intruder state difficulties. In the 2¹B_{1u} state of benzene, on the other hand, ESMP2 is energetically very similar to CASPT2, which is known to be highly accurate for the low-lying excitations of benzene,^{33,35,36} and so this appears to be a case where ESMP2 is reasonably accurate, at least if CASPT2 is used as the reference. Indeed, the MAD of ESMP2 relative to CASPT2 across all twelve states is significantly lower than its MAD relative to δ -CR-EOM-CC(2,3), which is perhaps not so surprising given that both ESMP2 and CASPT2 are second-order perturbation theories based on orbital-optimized reference functions (although for CASPT2 the orbital optimization is state-averaged, rather than state-specific). However, the agreement is certainly not perfect, and the large deviations between ESMP2 and δ -CR-EOM-CC(2,3) in the benzene 1¹B_{2u} and pyrimidine 1¹B₁ states cannot be explained by either similarity to CASPT2 or by intruder state issues in CASPT2, which were not present. The errors in these two states are likely due instead to doubly excited character that the singly-excited ESMF reference function cannot capture. Indeed, the doubly excited fractions of the CASSCF wave functions for benzene 1¹B_{2u} and pyrimidine 1¹B₁ were 15% and 8%, respectfully. It is interesting to note that, at least

TABLE VII: Size intensity test, in which we report the first singlet excitation energy in eV for a water molecule surrounded by a variable number of distant He atoms. Methods’ asymptotic cost scalings are given in parentheses.

He atoms	ESMF (N ⁴)	ESMP2 (N ⁵)	ESMP2 (N ⁷)	EOM-CCSD (N ⁶)	CISD (N ⁶)
0	7.7286	8.4508	8.4353	8.1946	10.1593
1	7.7286	8.4508	8.4353	8.1946	10.5369
2	7.7286	8.4508	8.4353	8.1946	10.9118
3	7.7286	8.4508	8.4353	8.1946	11.2841
4	7.7286	8.4508	8.4353	8.1946	11.6537
5	7.7286	8.4508	8.4353	8.1946	12.0207
6	7.7286	8.4508	8.4353	8.1946	12.3852

in these two cases, this modest fraction of doubly excited character caused less trouble for EOM-CCSD. This raises the interesting question of whether, for cases with modest amounts of doubly excited character, EOM-CCSD is more robust than ESMP2, which seems like a question worth studying more systematically in future work.

E. Rydberg Excitations

To check whether ESMP2 achieves a similar quality in Rydberg excitations, we have tested it on relevant excitations in neon, formaldehyde, and benzene. Although the comparison is less straightforward than those of the previous sections due to a lack of a single high-level benchmark, comparisons to literature values are shown in Table VI. We find that the overall accuracy for ESMP2 is similar to that seen in the ring systems above and that it makes a substantial correction to the uncorrelated ESMF reference, which in most cases underestimates these excitations (although interestingly not in neon).

F. Size Intensive Excitation Energies

Finally, although ESMP2 is rigorously size intensive — by which we mean that the excitation energy is unchanged by adding a second, infinitely-far-away system that does not participate in the excitation — it is worth testing that this property has been realized in our implementation. To this end, we treated a water molecule with various numbers of far-away helium atoms in a 6-31G basis. We performed seven calculations, one with just the water molecule and then six more, each with one additional He atom placed 10 Å away from the water at the different points of an octahedron. As seen in Table VII, the ESMP2 prediction for the excitation energy was unchanged by the addition of the He atoms, both for the original N⁷-scaling approach and the N⁵-scaling approach introduced here in which only the dominant TOP is considered large. While ESMP2’s size intensity is a formal advantage over CASPT2, which is only approximately size consistent,³⁷

CASPT2’s size intensivity error turns out to be less than 10^{-6} eV in this example. In contrast, the excitation energy of configuration interaction with singles and doubles (CISD), which is not even approximately size consistent or intensive, changes significantly upon adding the He atoms, despite the fact that they have essentially no interaction with the water molecule. This alarming behavior is a reminder of why size-intensivity is such a high priority in excited state methods, as artificial energy shifts of the size displayed here by CISD could spoil predictions of solvation properties such as solvatochromic shifts.

IV. CONCLUSION

We have shown that, by working in an orbital basis similar to that of the natural transition orbitals and by making a small modification to the zeroth order Hamiltonian, the cost scaling of the ESMP2 correction to the ESMF energy can be lowered from the seventh to the fifth power of the system size. In particular, the scaling matches the $N_o^2 N_v^3$ scaling of ground state MP2 theory, although the prefactor remains significantly higher due to the off-diagonal nature of ESMP2’s zeroth order Hamiltonian, which necessitates an iterative solution to the central linear equation. Initial testing of this lower-scaling incarnation of ESMP2 theory shows that its accuracy remains competitive with EOM-CCSD in many scenarios, but that it may break down more rapidly when doubly excited character is present. Given that this approach to ESMP2 gives it a lower cost-scaling than EOM-CCSD, these findings strongly motivate more systematic and widespread testing in future. The potential for a low-scaling method that is robust in charge transfer contexts is especially strong, as DFT still struggles in this area and modeling these systems reliably often requires the explicit inclusion of solvent species and can thus easily entail hundreds of atoms.

Going forward, the immediate priority is to work towards a production-level implementation of the most expensive terms within the theory. Happily, our automatic code-generation and cost-analysis has revealed that the number of terms with fifth order scaling is relatively small, and so a hand-tuned implementation employing dense linear algebra should be quite feasible. Once the practical efficiency of the implementation is addressed, it will be important to test the method in a significantly larger and more systematic set of excitations in order to more firmly establish in which contexts ESMP2 can be used as a lower-cost alternative to EOM-CCSD and in which contexts it cannot. Looking a bit farther ahead, it would be interesting to further exploit locality. The new approach here derives its scaling from the fact that molecular excitations’ spatial extents typically do not grow indefinitely with system size, but it does not exploit localities of electron correlation in the way many ground state methods now do. Finally, the realization of an excited state analogue of MP2 theory at the same cost scaling further motivates the study of applying a cluster operator to the ESMF reference wave function, which would be an important step towards the type of systematically improvable hierarchy of correlation methods that Hartree Fock theory has long enjoyed.

ACKNOWLEDGMENTS

This work was supported by the National Science Foundation’s CAREER program under Award Number 1848012. The Berkeley Research Computing Savio cluster performed the calculations.

J.A.R.S. acknowledges that this material is based upon work supported by the National Science Foundation Graduate Research Fellowship Program under Grant No. DGE 1752814. Any opinions, findings, and conclusions or recommendations expressed in this material are those of the author(s) and do not necessarily reflect the views of the National Science Foundation.

- ¹Grimme, S.; Hansen, A.; Brandenburg, J. G.; Bannwarth, C. Dispersion-corrected mean-field electronic structure methods. *Chem. Rev.* **2016**, *116*, 5105–5154.
- ²Ziegler, T.; Seth, M.; Krykunov, M.; Autschbach, J.; Wang, F. On the relation between time-dependent and variational density functional theory approaches for the determination of excitation energies and transition moments. *J. Chem. Phys.* **2009**, *130*, 154102.
- ³Park, Y. C.; Krykunov, M.; Ziegler, T. On the relation between adiabatic time dependent density functional theory (TDDFT) and the Δ SCF-DFT method. Introducing a numerically stable Δ SCF-DFT scheme for local functionals based on constricted variational DFT. *Mol. Phys.* **2015**, *113*, 1636–1647.
- ⁴Zhao, L.; Neuscamman, E. Density Functional Extension to Excited-State Mean-Field Theory. *J. Chem. Theory Comput.* **2020**, *16*, 164.
- ⁵Filatov, M.; Shaik, S. A spin-restricted ensemble-referenced Kohn-Sham method and its application to diradicaloid situations. *Chem. Phys. Lett.* **1999**, *304*, 429–437.
- ⁶Kowalczyk, T.; Tsuchimochi, T.; Chen, P. T.; Top, L.; Van Voorhis, T. Excitation energies and Stokes shifts from a restricted open-shell Kohn-Sham approach. *J. Chem. Phys.* **2013**, *138*, 164101.
- ⁷Mori-Sánchez, P.; Cohen, A. J.; Yang, W. Localization and delocalization errors in density functional theory and implications for band-gap prediction. *Phys. Rev. Lett.* **2008**, *100*, 146401.
- ⁸Isborn, C. M.; Mar, B. D.; Curchod, B. F.; Tavernelli, I.; Martinez, T. J. The charge transfer problem in density functional theory calculations of aqueously solvated molecules. *J. Phys. Chem. B* **2013**, *117*, 12189–12201.
- ⁹Gledhill, J. D.; Peach, M. J. G.; Tozer, D. J. Assessment of tuning methods for enforcing approximate energy linearity in range-separated hybrid functionals. *J. Chem. Theory Comput.* **2013**, *9*, 4414–4420.
- ¹⁰Zhao, L.; Neuscamman, E. Excited State Mean-Field Theory without Automatic Differentiation. *arXiv* **2020**, 2002.00322.
- ¹¹Shea, J. A. R.; Neuscamman, E. Communication: A mean field platform for excited state quantum chemistry. *J. Chem. Phys.* **2018**, *149*, 081101.
- ¹²Shea, J. A. R.; Gwin, E.; Neuscamman, E. A generalized variational principle with applications to excited state mean field theory. *J. Chem. Theory Comput.* **2020**, *16*, 1526–1540.
- ¹³Møller, C.; Plesset, M. S. Note on an approximation treatment for many-electron systems. *Phys. Rev.* **1934**, *46*, 618.
- ¹⁴Head-Gordon, M. An improved semidirect MP2 gradient method. *Mol. Phys.* **1999**, *96*, 673–679.
- ¹⁵Martin, R. L. Natural transition orbitals. *J. Chem. Phys.* **2003**, *118*, 4775.
- ¹⁶Head-Gordon, M.; Rico, R. J.; Oumi, M.; Lee, T. J. A doubles correction to electronic excited states from configuration interaction in the space of single substitutions. *Chem. Phys. Lett.* **1994**, *219*, 21–29.
- ¹⁷Li, C.; Verma, P.; Hannon, K. P.; Evangelista, F. A. A low-cost approach to electronic excitation energies based on the driven similarity renormalization group. *J. Chem. Phys.* **2017**, *147*, 074107.
- ¹⁸Roos, B. O.; Linse, P.; Siegbahn, P. E.; Blomberg, M. R. A. A simple method for the evaluation of the second-order-perturbation energy from external double-excitations with a CASSCF reference wavefunction. *Chem. Phys.* **1982**, *66*, 197–207.
- ¹⁹Andersson, K.; Malmqvist, P.-Å.; Roos, B. O. Second-order perturbation theory with a complete active space self-consistent field reference function. *J. Chem. Phys.* **1992**, *96*, 1218–1226.

- ²⁰Angeli, C.; Cimiraglia, R.; Evangelisti, S.; Leininger, T.; Malrieu, J.-P. Introduction of n -electron valence states for multireference perturbation theory. *J. Chem. Phys.* **2001**, *114*, 10252–10264.
- ²¹Riplinger, C.; Neese, F. An efficient and near linear scaling pair natural orbital based local coupled cluster method. *J. Chem. Phys.* **2013**, *138*, 034106.
- ²²Piecuch, P.; Hansen, J. A.; Ajala, A. O. Benchmarking the completely renormalised equation-of-motion coupled-cluster approaches for vertical excitation energies. *Mol. Phys.* **2015**, *113*, 3085–3127.
- ²³Piecuch, P.; Kucharski, S. A.; Kowalski, K.; Musiał, M. Efficient computer implementation of the renormalized coupled-cluster methods: The R-CCSD[T], R-CCSD(T), CR-CCSD[T], CR-CCSD(T) approaches. *Comput. Phys. Commun.* **2002**, *149*, 71–96.
- ²⁴Piecuch, P.; Gour, J. R.; Włoch, M. Left-eigenstate completely renormalized equation of motion coupled-cluster methods: Review of key concepts, extension to excited states of open-shell systems and comparison with electron-attached and ionized approaches. *Int. J. Quantum Chem.* **2009**, *109*, 3268–3304.
- ²⁵Kowalski, K.; Piotr, P. New coupled-cluster methods with singles, doubles, and noniterative triples for high accuracy calculations of excited electronic states. *J. Chem. Phys.* **2004**, *120*, 1715–1738.
- ²⁶Schmidt, M. W.; Baldridge, K. K.; Boatz, J. A.; Elbert, S. T.; Gordon, M. S.; Jensen, J. H.; Koseki, S.; Matsunaga, N.; Nguyen, K. A.; Su, S.; Windus, T. L.; Dupuis, M.; Montgomery, J. A. General Atomic and Molecular Electronic Structure System. *J. Comput. Chem.* **1993**, *14*, 1347–1363.
- ²⁷Barca, G. M. J. et al. Recent developments in general atomic and molecular electronic structure system. *J. Chem. Phys.* **2020**, *152*, 154102.
- ²⁸Shao, Y. et al. Advances in molecular quantum chemistry contained in the Q-Chem 4 program package. *Mol. Phys.* **2015**, *113*, 184–215.
- ²⁹Werner, H.-J.; Knowles, P. J.; Knizia, G.; Manby, F. R.; Schütz, M. Molpro: a general-purpose quantum chemistry program package. *Wiley Interdiscip. Rev. Comput. Mol. Sci.* **2012**, *2*, 242–253.
- ³⁰Werner, H.-J. Third-order multireference perturbation theory The CASPT3 method. *Mol. Phys.* **1996**, *89*, 645–661.
- ³¹Celani, P.; Werner, H.-J. Multireference perturbation theory for large restricted and selected active space reference wave functions. *J. Chem. Phys.* **2000**, *112*, 5546–5557.
- ³²Johnson, R. D. NIST Computational Chemistry Comparison and Benchmark Database. 2019; <http://cccbdb.nist.gov/>.
- ³³Loos, P.-F.; Lipparini, F.; Boggio-Pasqua, M.; Scemama, A.; Jacquemin, D. A Mountaineering Strategy to Excited States: Highly-Accurate Energies and Benchmarks for Medium Size Molecules. *J. Chem. Theory Comput.* **2020**, *16*, 1711–1741.
- ³⁴Falden, H. H.; Falser-Hansen, K. R.; Bak, K. L.; Rettrup, S.; Sauer, S. P. A. Benchmarking Second Order Methods for the Calculation of Vertical Electronic Excitation Energies: Valence and Rydberg States in Polycyclic Aromatic Hydrocarbons. *J. Phys. Chem. A* **2009**, *113*, 11995–12012.
- ³⁵Lorentzon, J.; Malmqvist, P.-Å.; Fülcher, M.; Roos, B. O. A CASPT2 Study of the Valence and Lowest Rydberg Electronic States of Benzene and Phenol. *Theor. Chim. Acta* **1995**, *91*, 91.
- ³⁶Del Bene, J. E.; Watts, J. D.; Bartlett, R. J. Coupled-cluster calculations of the excitation energies of benzene and the azabenzenes. *J. Chem. Phys.* **1997**, *106*, 6051–6060.
- ³⁷van Dam, H. J.; van Lenthe, J. H.; Ruttink, P. J. Exact size consistency of multireference Møller–Plesset perturbation theory. *Int. J. Quantum Chem.* **1999**, *72*, 549–558.